tvst

https://doi.org/10.1167/tvst.8.6.36

Article

Topical Brimonidine or Intravitreal BDNF, CNTF, or bFGF Protect Cones Against Phototoxicity

Francisco J. Valiente-Soriano[1,*], Arturo Ortín-Martínez[1,2,*], Johnny Di Pierdomenico[1], Diego García-Ayuso[1], Alejandro Gallego-Ortega[1], Juan A. Miralles de Imperial-Ollero[1], Manuel Jiménez-López[1], María Paz Villegas-Pérez[1], Larry A. Wheeler[3], and Manuel Vidal-Sanz[1]

[1] Departamento de Oftalmología, Facultad de Medicina, Universidad de Murcia, e Instituto Murciano de Investigación Biosanitaria Virgen de la Arrixaca (IMIB-Arrixaca), Murcia, Spain
[2] Present Address: Donald K. Johnson Eye Institute, Krembil Research Institute, University Health Network, Toronto, ON, Canada
[3] Ophthalmology and Visual Science, University of Utah Health Sciences Center, Salt Lake City, UT, USA

Correspondence: Manuel Vidal-Sanz, Dpto Oftalmología, Facultad de Medicina. Edificio Departamental, Campus de Ciencias de la Salud, Universidad de Murcia, 30120 El Palmar, Murcia, Spain. e-mail: manuel.vidal@um.es
Francisco J. Valiente-Soriano, Dpto Oftalmología, Facultad de Medicina. Edificio Departamental, Campus de Ciencias de la Salud, Universidad de Murcia, 30120 El Palmar, Murcia, Spain. e-mail: fjvaliente@um.es

Received: 5 July 2019
Accepted: 7 October 2019
Published: 16 December 2019

Keywords: neuroprotection; cone photoreceptors; light induced phototoxicity; BDNF; bFGF; CNTF; Brimonidine; alpha-2-adrenergic agonist; microglia; SD-OCT

Citation: Valiente-Soriano FJ, Ortín-Martínez A, Di Pierdomenico J, García-Ayuso D, Gallego-Ortega A, Miralles de Imperial-Ollero JA, Jiménez-López M, Villegas-Pérez MP, Wheeler LA, Vidal-Sanz M. Topical brimonidine or intravitreal BDNF, CNTF, or bFGF protect cones against phototoxicity. Trans Vis Sci Tech. 2019;8(6):36, https://doi.org/10.1167/tvst.8.6.36

Purpose: To develop a focal photoreceptor degeneration model by blue light-emitting diode (LED)-induced phototoxicity (LIP) and investigate the protective effects of topical brimonidine (BMD) or intravitreal brain-derived neurotrophic factor (BDNF), ciliary neurotrophic factor (CNTF), or basic fibroblast growth factor (bFGF).

Methods: In anesthetized, dark-adapted, adult female Swiss mice, the left eye was dilated and exposed to blue light (10 seconds, 200 lux). After LIP, full-field electroretinograms (ERG) and spectral-domain optical coherence tomography (SD-OCT) were obtained longitudinally, and reactive-Iba-1$^+$monocytic cells, TUNEL$^+$ cells and S-opsin$^+$ cone outer segments were examined up to 7 days. Left eyes were treated topically with BMD (1%) or vehicle, before or right after LIP, or intravitreally with BDNF (2.5 μg), CNTF (0.2 μg), bFGF (0.5 μg), or corresponding vehicle right after LIP. At 7 days, S-opsin$^+$ cone outer segments were counted within predetermined fixed-size areas (PFA) centered on the lesion in both flattened retinas.

Results: SD-OCT showed a circular region in the superior-temporal left retina with progressive thinning (207.9 ± 5.6 μm to 160.7 ± 6.8 μm [7 days], $n = 8$), increasing TUNEL$^+$ cells (peak at 3 days), decreasing S-opsin$^+$ cone outer segments, and strong microglia activation. ERGs were normal by 3 days. Total S-opsin$^+$ cones in the PFA for LIP-treated and fellow-retinas were 2330 ± 262 and 5601 ± 583 ($n = 8$), respectively. All neuroprotectants ($n = 7$–11), including topical BMD pre- or post-LIP, or intravitreal BDNF, CNTF, and bFGF, showed significantly greater S-opsin$^+$ cone survival than their corresponding vehicle-treated groups.

Conclusions: LIP is a reliable, quantifiable focal photoreceptor degeneration model. Topical BMD or intravitreal BDNF, CNTF, or bFGF protect against LIP-induced cone-photoreceptor loss.

Translational Relevance: Topical BMD or intravitreal BDNF, CNTF, or bFGF protect cones against phototoxicity.

Introduction

Age-related macular degeneration (AMD) causes a gradual degeneration of cones located in the human macula and is the most common cause of blindness in elderly people.[1] In addition to environmental factors, such as smoking, hypertension, or obesity, light may be an important risk factor of AMD at early stages.[2] Several animal models that mimic human retinal degenerations are studied in order to foster our understanding of AMD, including (1) spontaneous or induced genetic alterations, such as the Royal College of Surgeons rat, the P23H rat or the rd mouse[3–13]; (2) chemically induced retinal degenerations, such as poisoning with sodium iodate[14–17] or N-methyl-N-nitrosurea,[18,19] and; (3) light-induced retinal degeneration by phototoxicity.[20–28] Blue light is of interest, because it has proven to induce retinal damage through an oxidative stress mechanism leading to retinal pigment epithelium (RPE) and photoreceptor loss,[29–31] and thus is considered a risk factor for AMD.[32–34] Recent studies using a blue light-emitting diode (LED) to expose the retina in albino[26,35] or pigmented[27] mice results in massive photoreceptor degeneration throughout the entire retina, as well as RPE damage.[27] These studies implicated long time intervals of exposure and large intensities (2 hours, 400–1100 Lux[27,35]; 3 hours 1000–6000 lux[26]; 24 hours 6000 Lux[28]) of blue LED light, and thus there are no models of acute and focal damage to the retina to investigate the effects of blue LED damage and rescue.

Several studies have documented the efficacy of neurotrophic factors in promoting neuronal survival following diverse types of injuries.[36] Indeed, the rodent retina provides an ideal model to investigate the short- and long-term responses and neuroprotection against a variety of diseases or injuries, such as axotomy,[37–40] transient ischemia of the retina induced by elevated intraocular pressure,[41] or by selective ligature of the ophthalmic vessels,[42,43] glaucomatous damage induced by chronic[44] or acute[45] elevation of the intraocular pressure, and inherited[46] or phototoxicity-induced[47] retinal degenerations. Moreover, we have previously demonstrated that brain-derived neurotrophic factor (BDNF) and basic fibroblast growth factor (bFGF) protect cone-photoreceptors against LED-induced focal retinal damage in adult rats.[25] However, ciliary neurotrophic factor (CNTF) was ineffective,[25] although its neuroprotective effect has been contrasted in other retinal degenerations.[48] In addition, previous studies have shown that brimonidine (BMD) has neuroprotective effects against transient ischemia of the retina-induced neuronal death[41,49,50] and LED-induced phototoxicity (LIP)-induced retinal degeneration.[25]

Most of the previous studies investigating neuroprotection afforded against light-induced phototoxicity describe the effects on rod photoreceptors.[26–28,35] There is however, little information regarding cone photoreceptor survival.[25] Rodents do not have a proper macula; however, we have previously described an "arciform photosensitive area" in the rat retina,[21–23,47] which coincides with the visual streak described in the dorsal retina in rats and mice,[51–55] with highest densities of retinal ganglion cells and L-cones in the superior-temporal region,[56] that is probably a specialized region of the retina to provide best visual acuity. In the albino mice, approximately 73% of cones are dual, 23% are genuine S-cones, and 4% are genuine L-cones; thus, immunodetection of the S-opsin identifies approximately 96% of the whole population of cones.[55]

Here, we aimed to establish a novel reproducible and reliable model of blue LIP that results in a focal circumscribed lesion of photoreceptors centered in the temporal side of the visual streak in the albino mice. We have examined longitudinally in vivo retinal thinning and function with spectral-domain optical coherence tomography (SD-OCT) and full-field electroretinography (ERG), respectively, and ex vivo we have quantified the effects on the survival of the population of S-opsin$^+$ cone outer segments and observed the microglial reaction and the presence of apoptosis. Our studies document that LIP is a reproducible and reliable model to study focal photoreceptor degeneration in mice. In addition, we demonstrate that topical BMD or intravitreal BDNF, CNTF, or bFGF may prevent, at least in part, light-induced cone photoreceptor degeneration. Short accounts were presented in abstract format (Vidal-Sanz M, et al., *IOVS* 2015;55:ARVO E-Abstract 5667).

Material and Methods

Animal Handling

All experiments followed the ARVO and European Union guidelines for the use of animals in research and were approved by the Ethical and Animal Studies Committee (University of Murcia [UM]). Adult female albino Swiss mice (25–30 g) were obtained

from Charles River Laboratories (L'Arbresle, France) and housed at the UM animal facilities in temperature and light controlled rooms (12-hour light/dark cycle) with food and water ad libitum. For surgical or animal manipulations, mice were anaesthetized with an intraperitoneal (ip) injection of ketamine (70 mg/kg Ketolar; Pfizer, Alcobendas, Madrid, Spain) and xylazine (10 mg/kg Rompun; Bayer, Kiel, Germany). Topical ointment (Tobrex; Alcon-Cusí, S.A., El Masnou, Barcelona, Spain) was applied during recovery to prevent corneal desiccation. Mice were euthanized with pentobarbital (Dolethal, Vetoquinol; Especialidades Veterinarias, S.A., Alcobendas, Madrid, Spain). In the present experiments we have used six naïve untouched mice, and 110 subjected to LIP; their left eyes were used as experimental while the right eyes served as controls. Because our previous studies characterizing the cone population of adult mice were done in female mice,[55] for comparison we have used only female mice in the present study.

Light-Emitting Diode Induced–Phototoxicity (LIP)

Light damage differs between rats[22,25] and mice[24] and thus different light protocols are needed for light-induced retinal degeneration. Light-induced retinal phototoxicity depends on the type of light employed, radiation intensity, wavelength, and exposure time intervals.[20,57] Because short wavelengths are known to cause severe damage, here we have used a blue LED.[28,58–60] Mice were dark-adapted for 12 hours[61] and the left eye was dilated with tropicamide (Tropicamida 1%; Alcon-Cusí, S.A., El Masnou) 1 hour prior to LIP. Mice heads were placed on a head-holder and a 10-V blue LED (emission spectrum 390–410 nm; catalogue number 454–4405; Kingbright Elec. Co., Taipei, Taiwan) was placed at 1 mm from the corneal apex of the left eye. The duration of exposure and illuminance were controlled by a computer connected to the LED. Preliminary experiments showed consistent results after exposing mice to 200 lux for 10 seconds, with light focused always on the same area of the retina. Lux intensity was controlled with a luxometer (light meter TES-1330; TES Electrical Electronic Corp., Taipei, Taiwan). This LED produces blue radiation, which causes retinal excitotoxicity[62] and has proven effective in a previously characterized model of focal phototoxicity in adult albino rats.[25] LIP was always performed at the same hour (10:00 AM to 12:00 PM) to minimize retinal susceptibility to light damage influenced by the circadian rhythm.[57,61,63]

Spectral-Domain Optical Coherence Tomography (SD-OCT)

The effects of LIP were characterized in vivo longitudinally in the retinas of two naïve ($n = 4$ retinas) and eight LIP-treated anesthetized mice ($n = 8$ retinas) using a SD-OCT device (Spectralis; Heidelberg Engineering, Heidelberg, Germany) as described.[25] Retinal thickness (from the fiber layer to the RPE) in the center of the lesion was measured pre-, 1, 2, 3, 5, and 7 days after LIP using the average of three measurements of calipers provided directly by the software of the device.

Electroretinography (ERG)

The effects of LIP were analyzed in vivo longitudinally in both retinas of four LIP-treated mice using full-field ERG as described.[64,65] In brief, in anesthetized dark-adapted mice, both eyes were stimulated with increasing light stimuli (–4.4 to 2 log cd·s/m^2), provided by a Ganzfeld dome light. ERG responses were recorded by Burian-Allen bipolar electrodes located on both corneas, protected with methylcellulose (Methocel 2%; Novartis Laboratories CIBA Vision, Annonay, France), a reference electrode was also placed in the mouth and the ground electrode was a needle placed subcutaneously at the base of the tail. Electrical signals were digitized using a Power Lab data acquisition board (AD Instruments, Chalgrove, UK). Standard ERG waves were analyzed according to the method recommended by the International Society of Clinical Electrophysiology of Vision.

Administration of the Neuroprotective Compounds

Neuroprotection against S-cone photoreceptor loss was examined for noninvasive topical or intravitreal administration of neuroprotective compounds. The effects of alpha-2-adrenergic agonist, BMD, were studied in two groups. Two (2.5 µL) drops of 1% BMD (Allergan Inc., Irvine, CA) in 0.9% NaCl were administered topically three times a day; in one group, BMD treatment started the day before LIP (pre-LIP group; $n = 11$) and in the other BMD was instilled immediately after LIP (post-LIP group; $n = 7$). We also tested three neurotrophic factors intravitreally injected right after LIP, 2.5 µL containing 2.5 µg of BDNF (Preprotech, London, UK) ($n = 8$), or 0.2

Table. Total Numbers of S-Opsin$^+$ Outer Segments Automatically Quantified in the Fixed-Size Areas

Parameter	*n*	Area	Mean ± SD
No treatment	8	R	5601 ± 583
		L	2330* ± 262
Topical administration			
Saline PRE	13	R	6053 ± 672
		L	2247* ± 858
BMD PRE	11	R	5993 ± 987
		L	3527*† ± 556
Saline POST	7	R	5923 ± 872
		L	2040* ± 773
BMD POST	7	R	5532 ± 594
		L	3777*† ± 900
Intravitreal administration			
PBS	9	R	5911 ± 1271
		L	1703* ± 665
BDNF	8	R	5057 ± 610
		L	3365*† ± 558
CNTF	7	R	5448 ± 1369
		L	3245*† ± 1116
TRIS	7	R	6136 ± 933
		L	2179* ± 525
bFGF	7	R	6135 ± 950
		L	3650*† ± 786

Comparison of the total numbers of S-opsin$^+$ outer segments automatically quantified in the fixed-size areas (radius of 0.4 mm) located in the center of the LED induced lesion for the left retinas and in a corresponding region for the right retinas. All left areas (L) show a significative reduction of positive cones compared to their right control areas (R) (Mann–Whitney test, $^*P < 0.05$). Also, left areas treated topically with brimonidine before and just after LED photoexposition or treated intravitreally with BDNF, CNTF or bFGF show a significative protection of S-cones compared to their corresponding vehicle treated left areas (Mann–Whitney test, $^\dagger P < 0.05$).

µg of CNTF (R&D Systems, Vitro S.A. Madrid, Spain) ($n = 7$), both diluted in phosphate buffered saline (PBS), or 0.5 µg of bFGF (Preprotech) ($n = 7$) diluted in Tris-Cl 2 mM pH 7.6. As controls, mice treated with each vehicle solution at the same frequency and route than the experimental groups were used ($n = 7$–13). All animals were analyzed 7 days after LIP (Table).

Tissue Processing

Mice were deeply anesthetized and perfused transcardially with saline and 4% paraformaldehyde in 0.1 M phosphate buffer at 1, 2, 3, 5, or 7 days after LIP. Both eyes were enucleated[38,66–68] and all retinas prepared as whole-mounts following a standard protocol in our laboratory.[25,54,69–72]

Immunohistofluorescence

To study cone photoreceptor damage and its protection, S-opsin antibody (goat anti-OPN1SW; 1:1,000; Santa Cruz Biotechnologies, Heidelberg, Germany) detected with Alexa Fluor-594 donkey anti-goat (1:500; IgG [H+L]; Molecular Probes, Invitrogen, ThermoFisher, Madrid, Spain) was used to immunodetect S-cones, which represent 96% of all cones.[25,54]

To study the microglial reaction (microglia and recruited macrophages) in untouched naïve mice ($n =$ 2, 4 retinas) and at 1, 3, 5, or 7 days ($n = 4$ per time) after LIP, the left experimental, LED exposed, and the contralateral unexposed retinas were doubly immunodetected with S-opsin antibodies and ionized calcium binding adaptor molecule (Iba-1) antibodies (1:500; rabbit anti-Iba1, EPR16589; ABCAM, Cambridge, UK) and counterstained with 4′,6-diamidino-2-phenylindole (DAPI). Secondary antibody for Iba-1 was Alexa Fluor-488 donkey anti-rabbit IgG (1:500; Molecular Probes, Invitrogen, ThermoFisher, Madrid, Spain).

To assess whether S-opsin$^+$ outer segments loss was due to apoptosis and not to S-opsin downregulation, both whole-mounted retinas underwent a TdT-mediated dUTP nick-end labeling (TUNEL) assay, immunolabelling for S-opsin, and counterstaining with DAPI at 1, 2, 3, 5, or 7 days ($n = 3$ per time) after LIP and also in untouched naïve mice ($n = 2$, 4 retinas). To detect apoptotic nuclei, TUNEL assay (FragEL DNA Fragmentation Detection Kit; Qiagen, Merck Bio, Nottingham, UK) was performed as described[11,22] with minor modifications.

Retinal Analysis

All retinal wholemounts were examined and photographed with a microscope (Axioscop 2 Plus; Zeiss, Jena, Germany) following a standard protocol.[25,39,70] Iba-1$^+$cells and TUNEL$^+$ cells were examined in wholemounts and photographed using a Leica SP8 confocal microscope (×20, ×40, or ×63; Leica Microsytems, Wetzlar, Germany). Images were further processed using a graphics editing program when required (Adobe Photoshop CS 8.0.1; Adobe Systems, Inc., San Jose, CA). Photomontages of wholemounts were constructed from 154 consecutive frames

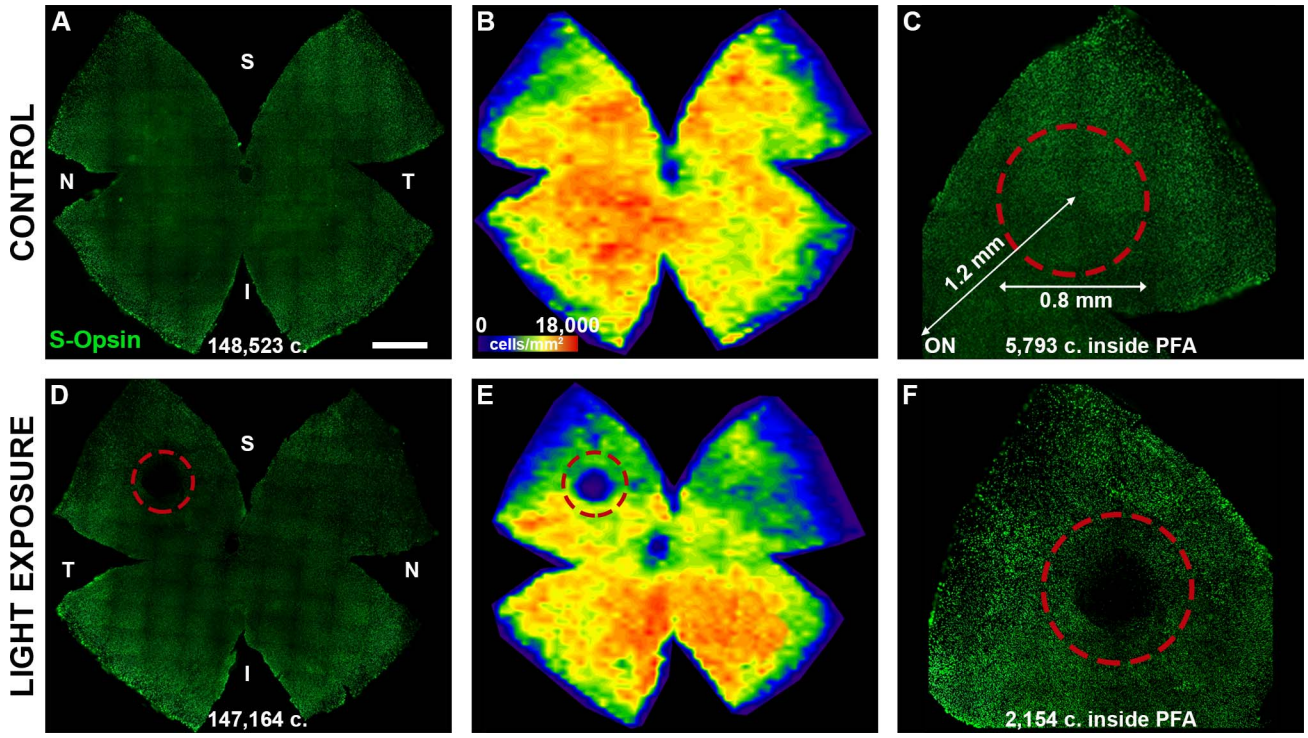

Figure 1. Focal loss of S-cones. Whole-mount of a control (contralateral unexposed) (A) and the experimental (D) mouse retina analyzed 7 days after LIP showing S-cone immunodetection, its corresponding isodensity maps (B, E) and photomontages of the superior-temporal retinal quadrants depicting the analyzed/damaged area (C, F). (A, B) The total number of S-cones (c.) and their normal distribution in control retinas; (D, E) this distribution is altered within a small circular region (focal damaged area) of S-cone degeneration after LIP. The damaged area after LIP could be seen in the superior-temporal quadrant (D, E) and in the magnification of this quadrant ([F]; outlined in the *red dotted circle*). (C) Illustrates the predetermined fixed-size circular area (PFA) outlined in the *red dotted circle* (diameter of 0.8 mm) circumscribing the focal lesion that was analyzed in control (contralateral unexposed) and experimental retinas. This area was located at approximately 1.2 mm from the optic disc. Note that while the PFA in the control retina (C) contains 5793 S-opsin$^+$ cones, the experimental retina (F) only shows 2154. ON, optic nerve; S, superior; I, inferior; T, temporal; N, nasal. *Scale bar* = 500 μm.

captured side by side. Reconstructed images were further processed with image-editing computer software (Adobe Photoshop CS; ver. 8.0.1; Adobe Systems, Inc.) when correct orientation of the retina or image coupling was needed.[36,73,74]

Automatic Quantification of S-Cones in a Predetermined Fixed-Size Circular Area and Isodensity Maps

Total numbers of surviving S-cones were counted automatically using routines developed in our laboratory,[25,47,54,55,75] and isodensity maps were constructed (Sigmaplot 9.0; Systat Software Inc., Richmond, CA) for detailed S-cone topologic distribution.[25,54,55] The LIP retinas exhibited damage in a circular region within the superior-temporal quadrant whose center was located at approximately 1.2 mm from the optic nerve head. S-opsin$^+$ outer segments were counted within a predetermined PFA centered in the middle of the lesion with a radius of 0.4 mm (Fig. 1). These counts were done in the left (LIP-treated) and in the corresponding region of the right (fellow) retina for each mouse (Fig. 1).

Automatic Quantification of the Positive TUNEL Signal Area in a Predetermined Fixed-Size Circular Area

TUNEL$^+$ cells were examined in whole mounts using a Leica SP8 confocal microscope (×20), and the positive TUNEL signal was automatically quantified in a smaller predetermined circular area (radius = 0.25 mm) centered in the lesion delimiting the TUNEL expression using the commercial ImageJ software (National Institutes of Health, Bethesda, MD). This analysis was performed in untouched naïve mice (n = 3, 3 retinas) and at 1, 2, 3, 5, or 7 days (n = 3 per time) after LIP.

Statistical Analysis

Statistical analysis was done using GraphPad Prism (GraphPad Software, San Diego, CA). Tukey test or Kruskal–Wallis test were used when comparing more than two groups and Mann-Whitney U test when comparing two groups only. Data is shown as mean ± SD and differences were considered significant when $P < 0.05$.

Results

In Vivo Analysis of Retinal Damage Induced by LIP

In control mice, SD-OCT scans showed a mean retinal thickness of 207.9 ± 6 µm ($n = 12$; Fig. 2) in the superior-temporal area, coincident with the damaged area in experimental mice. In experimental animals, SD-OCT scans of the left retina showed retinal alterations in a circumscribed area of the superior-temporal quadrant that were evident upon inspection of the eye fundus (Fig. 2). Longitudinal SD-OCT measurements indicate a significant and progressive retinal thinning between 1 and 7 days after LIP (Tukey test, $P < 0.05$). By 1 day after LIP there was retinal thickness reduction (192.5 ± 7 µm, $n = 8$) that progressed until 7 days (2 days, 182.9 ± 6 µm; 3 days, 171.6 ± 6 µm; 5 days, 166.4 ± 7 µm; and 7 days, 160.7 ± 7 µm; $n = 8$) showing a significant exponential trend ($r^2 = 0.865$) (Fig. 2). Such retinal thinning was mainly due to outer nuclear and segment layer thinning. On days 1 and 2, the OCT images showed a hyperreflective material in the center of the lesion that encompassed the entire external retina without discriminating layers that resolved by day 3. It has been postulated that this type of nonspecific signal in the external retina may be due to a process of inflammation derived from light damage that causes an alteration in the Müller cells and an accumulation of debris from the external segments that causes a redistribution of the retinal fluid.[6,76–78] This edema can cause a barrier in the passage of OCT infrared light and generate a refractive change, which causes a nonspecific hyperreflective signal[76,77] (Fig. 2).

In Vivo Functional Analysis of Retinal Damage Induced by LIP

Longitudinal analyses of full-field ERGs from both retinas in LIP-exposed mice ($n = 4$) showed a significant reduction in retinal function on the left retina (decrease in response: a wave 26.5%, b wave 38.4%) within 24 hours of LIP, that recovered fully by 3 and 7 days (Fig. 3).

Immunocytochemical Analysis of the Damaged Region in Whole-Mounts: Focal Loss of S-Cones

The naïve and the right retinas of the LIP animals showed the typical distribution of S-opsin$^+$ cones.[55] In contrast to the pigmented strain, in which S-opsin$^+$ cones are located mainly in the ventral retina, albino mice S-opsin$^+$ cones are distributed homogeneously throughout the retina with higher densities in the dorsal and ventral retina (Fig. 1). The LIP-treated retinas showed, consistent with the in vivo SD-OCT observations, diminished S-opsin$^+$ outer segments in a small circular region (approximate diameter of 0.65 mm) located in the superior-temporal quadrant whose center was placed at approximately 1.2 mm from the optic disc (Fig. 1). Within this small circular area, there were diminished numbers of S-opsin$^+$ outer segments in the periphery and an almost complete absence in the center of the lesion (Fig. 1). Total numbers of S-opsin$^+$ outer segments in the LIP retinas and their fellow retinas were comparable (Mann-Whitney U test, $P > 0.05$), probably because of the small size of the lesion (data not shown). We then counted total S-opsin$^+$ outer segments within a predetermined fixed-size circular area (0.8-mm diameter, centered in the middle of the lesion) and found that the mean number of S-opsin$^+$ outer segments were 5601 ± 583 ($n = 8$) in the contralateral fellow retinas and 2330 ± 262 ($n = 8$) in the LIP exposed retinas, indicating a reduction of approximately 58% of the S-cone population (Fig. 1, Table).

Microglial Activation in the Focal Damaged Region

Double labeling with Iba-1 and S-opsin allowed to analyze the presence of active microglia and recruited macrophages and S-opsin$^+$ outer segments in control and experimental retinas (Fig. 4). In naïve or control retinas there were few to none Iba-1$^+$ cells within the outer nuclear and outer segment layer of the retina. However, in the experimental LIP treated retinas, a few Iba-1$^+$ cells were apparent delineating the boundaries of the area of lesion already at 1 day after LIP (Fig. 4), at a time when S-opsin immunoreactivity only showed shortening of the outer segments but no clear loss. By 3 days after LIP the highest numbers of cells Iba-1$^+$ were observed within

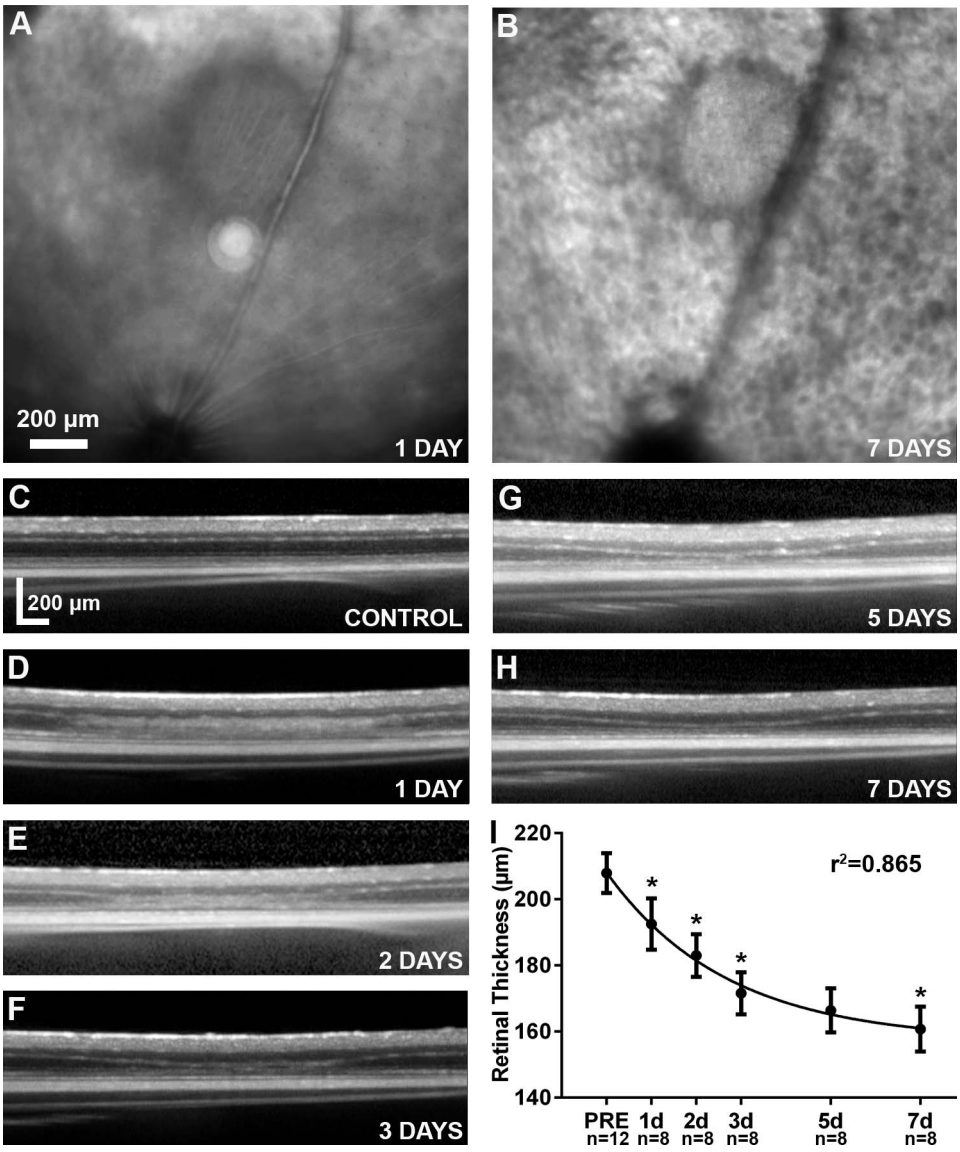

Figure 2. SD-OCT longitudinal in vivo retinal thickness analysis after LIP. (A, B) Eye fundus photographs acquired 1 and 7 days after LIP. Representative SD-OCT scans obtained from control-naïve mice retina (C) and from a representative experimental retina 1 (D), 2 (E), 3 (F), 5 (G), and 7 (H) days after LIP treatment on the left eye. (I) Exponential graph showing significant and progressive retinal thinning (mean ± SD) in the left LIP-treated retinas from 1 to 7 days in the analyzed area (Tukey test $*P < 0.05$; $r^2 = 0.865$).

the area of the lesion, whose center showed a clear diminution of S-opsin$^+$ outer segments. The microglial cell reaction was similar at 5 and 7 days after LIP (Fig. 4) but the number of S-opsin$^+$ outer segments continued decreasing. Confocal microscopy examination showed Iba-1$^+$ cells located mainly within the outer retinal layers (Fig. 4). The morphology of these microglia cells changed over time from a dendritic form on day 1 to an ameboid form on day 3. On day 7, Iba-1–positive cells showed a less amoeboid and more branched pattern.

Apoptotic Nuclei Within the Focal Damaged Area of the Retina

To assess whether S-opsin$^+$ outer segment loss was due to apoptosis and not a downregulation of the S-opsin expression, a TUNEL assay was performed in whole-mounted retinas at various time intervals after LIP and retinas were immunolabeled for S-opsin and counterstained with DAPI (Fig. 5). In control retinas, TUNEL-positive nuclei were not observed (Fig. 5). In the LIP-damaged retinas, TUNEL-positive nuclei

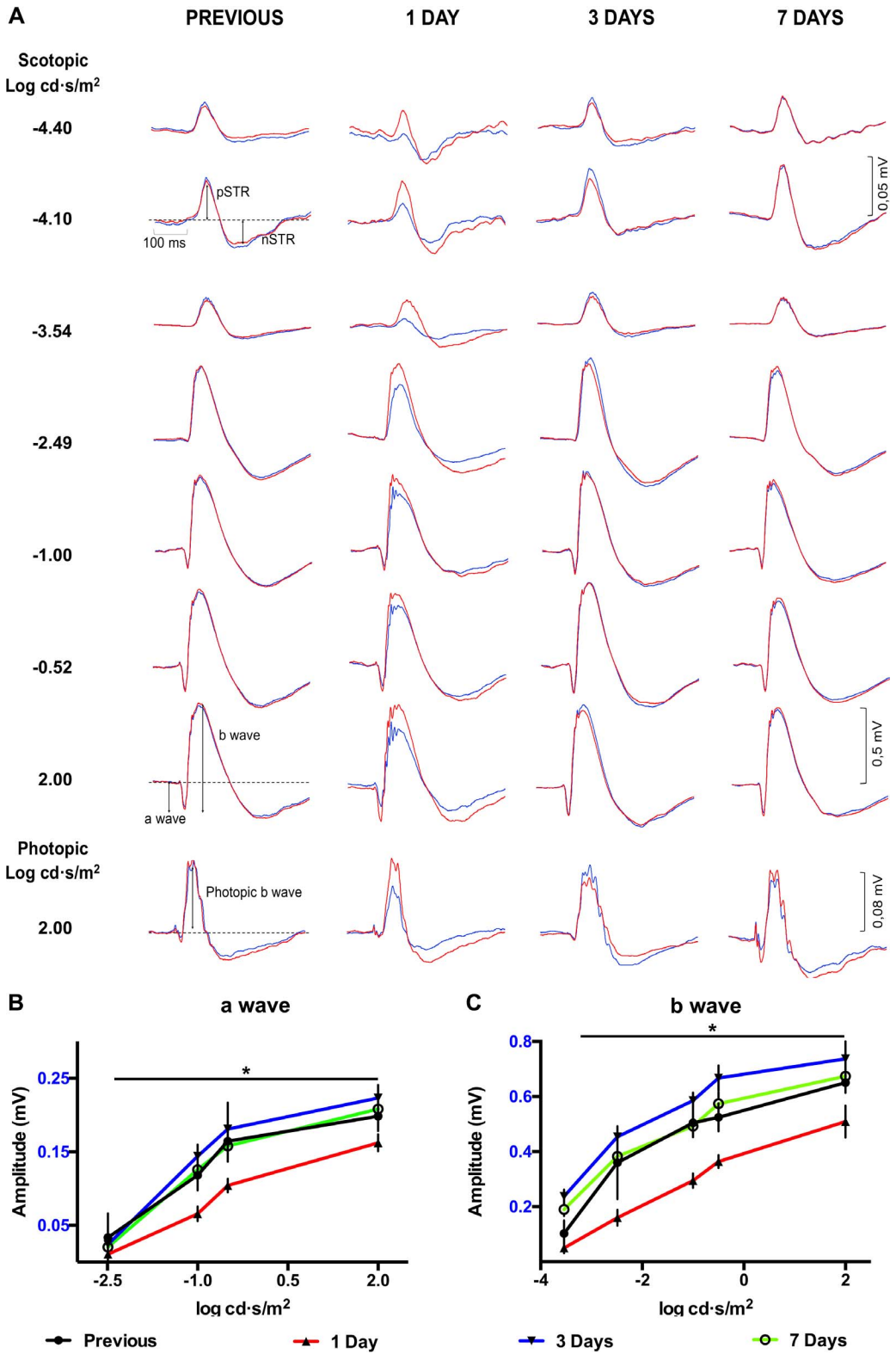

Figure 3. ERG response after LIP. (A) Full-field ERG representative trace recordings from previous, 1, 3, and 7 days after LIP in response to different increasing light intensities (*left margin*). *Blue lines* represent the left eye responses (LIP-treated), and *red lines* represent the right eye responses (contralateral noninjured). A significant reduction in a- and b-waves in scotopic and photopic light conditions was observed 24 hours after LIP. This temporal reduction recovered fully at 3 days and the responses kept normal until day 7. (B, C) Line →

←
graphs representing the a- and b-wave amplitudes (mV) from the longitudinal ERG study on the previous, 1, 3, and 7 days after LIP ($n = 4$) (x axis for a wave: from −2.49 to 2 log cd·s/m^2; x axis for b wave: from −3.54 to 2 log cd·s/m^2). Data shown as mean ± SD; *$P < 0.01$ (Previous versus day 1; one-way ANOVA post hoc Dunnett's).

were only detected within the outer nuclear layer. A few TUNEL-positive nuclei were apparent as early as 1 day after LIP occupying 11% of the small predetermined circular area. Their number increased rapidly by 2 days reaching a peak by 3 days after LIP (occupying 62% and 79% of the small predetermined circular area, respectively; Fig. 5). By 5 and 7 days the number of TUNEL-positive nuclei diminished but were still noticeable (occupying 45% and 21% of the small predetermined circular area, respectively; Fig. 5). A parallel qualitative examination demonstrated a progressive diminution in the numbers of S-opsin$^+$ outer segments. By 1 day after LIP there were already signs of lesioned S-opsin$^+$ outer segments, which appeared shortened (data not shown). The progressive diminution in numbers of S-opsin$^+$ outer segments revealed with clarity the boundaries of the phototoxic lesion; becoming clearer by 2 and 3 days, and obvious by 5 and 7 days when very few S-opsin$^+$ outer segments were left in the center of the lesioned area (Fig. 5).

Prevention of LED-Induced Cone Loss With Topical BMD or Intravitreal BDNF, CNTF, or bFGF

BMD was topically administered just before or right after LIP and the mean population of S-opsin$^+$ outer segments were quantified in the PFA of the LIP-treated and their fellow retinas (Fig. 6, Table). In the groups of animals treated before or right after LIP with BMD, the mean number of S-opsin$^+$ outer segments were 3527 ± 556 (mean ± SD; $n = 11$) or 3777 ± 900 ($n = 7$), respectively. These numbers were significantly greater than those found in the groups of animals treated before or right after LIP with saline (vehicle group), 2247 ± 858 ($n = 13$), or 2040 ± 773 ($n = 7$), respectively. Thus, topical BMD afforded a significant neuroprotection of the of S-cone population compared with vehicle-treated animals, and this effect was obtained independently of whether BMD was administered before or immediately after LIP (Fig. 7, Table).

The effects of BDNF (2.5 μg), CNTF (0.2 μg), or bFGF (0.5 μg) administered intravitreally right after LIP were also quantified in the PFA of the LIP-treated and their fellow retinas (Fig. 6). Intravitreal injection of BDNF or CNTF resulted in 3365 ± 558 ($n = 8$) or 3245 ± 1116 ($n = 7$) S-opsin$^+$ outer segments, respectively, and these were significantly greater than those found in animals treated intravitreally with PBS (vehicle; 1703 ± 665; $n = 9$). Intravitreal injection of bFGF resulted in 3650 ± 786 ($n = 7$) S-opsin$^+$ outer segments while intravitreal injection of TRIS (vehicle) resulted in significantly smaller number of S-opsin$^+$ outer segments (2179 ± 525; $n = 7$) (Fig. 7, Table). Thus, all the studied neurotrophic factors showed significant neuroprotection of the S-cone population when compared with their corresponding vehicle-treated animals (Fig. 7).

Discussion

The present studies in adult Swiss mice were designed to address the following three main questions: (1) Does blue LIP result in a reproducible focal loss of cones? (2) Does LIP induce apoptosis of photoreceptors and microglial reaction? (3) Can the photoreceptor damage be blunted with the use of neuroprotective substances by topical or intravitreal administration? We used techniques developed in the laboratory to identify and count automatically the population of S-cone-photoreceptors and represent their topographic distribution with isodensity maps, in control and experimental conditions. Our results indicate that LIP results in a reproducible and quantifiable model of focal phototoxic cone degeneration in albino mice. SD-OCT longitudinal in vivo analysis showed progressive thinning of the outer retina from 1 to 7 days after LIP, in a small circumscribed area of the superior-temporal quadrant. ERG longitudinal in vivo analysis showed a transient diminution in retinal function (a- and b-waves) that recovers fully by 3 days and is maintained by 7 days after LIP. Focal damage was confirmed by the presence of activated microglia and recruited macrophages cells and TUNEL-positive cells, indicating that LIP courses with photoreceptor apoptosis. Detailed quantification showed, within the focal lesion, the loss of approximately 58% of the S-opsin$^+$ outer segments, an effect that could be prevented

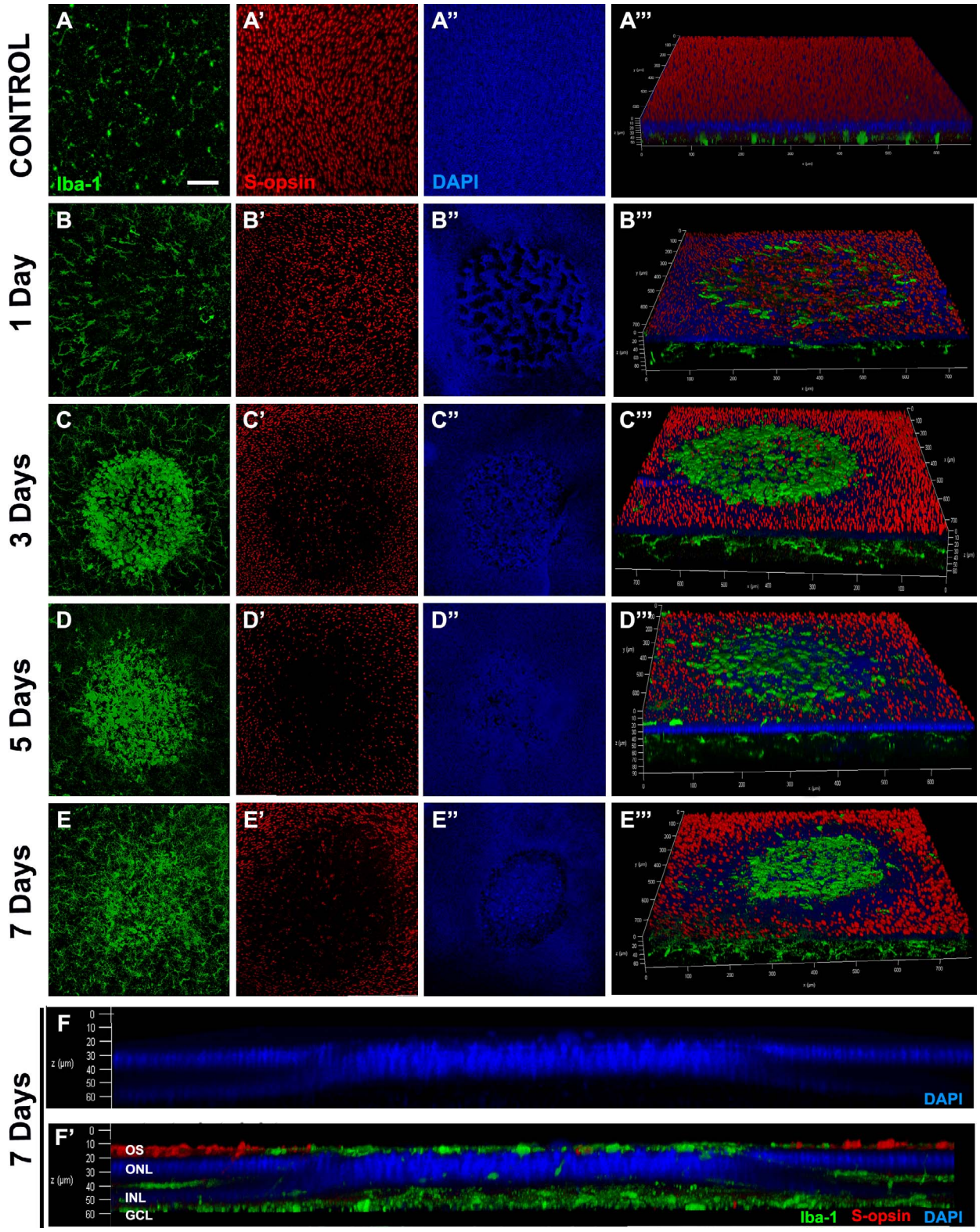

Figure 4. Microglial activation after LIP. Confocal magnification of a control retina and of the damaged area at 1, 3, 5, or 7 days after LIP showing microglia (A–E), S-opsin^{+} cones (A'– E'), and DAPI counterstaining (A''–E''). (A'''–E''') Merged images. Microglial reaction was observed within the outer retinal layers in an area coincident with the damaged area as can be observed in DAPI image (F) and stained against microglia and S-opsin (F'). Microglial reaction is higher 3 days after LIP and is maintained between 5 and 7 days after LIP. OS, outer segments; ONL, outer nuclear layer; INL, inner nuclear layer; GCL, ganglion cell layer. *Scale bar* = 100 µm.

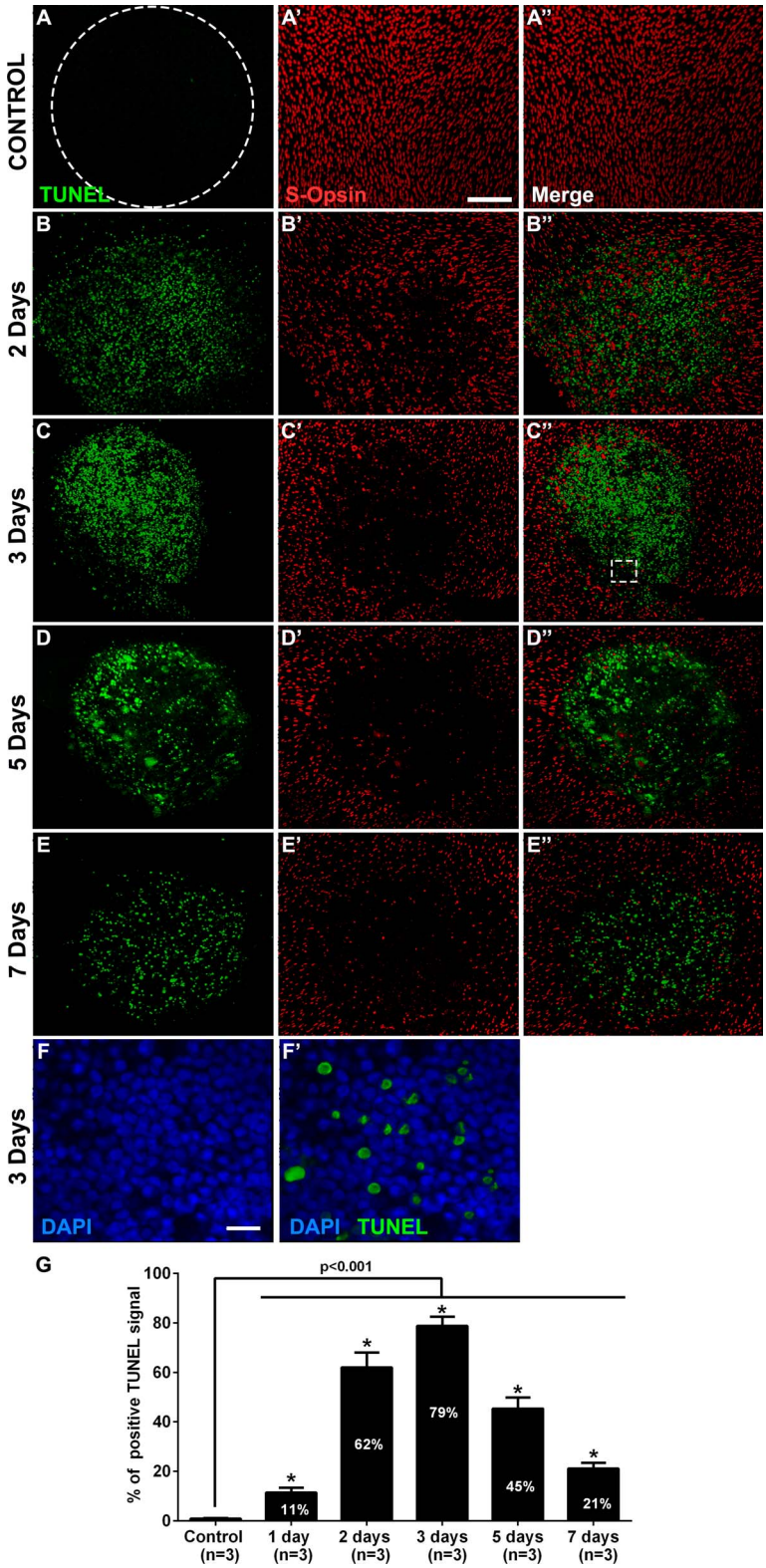

Figure 5. LIP induced apoptotic cell loss. Magnification of a control retina and of the damaged area showing TUNEL-positive nuclei (A–E) and S-opsin^{+} cones (A′–E′) at 2, 3, 5, or 7 days after LIP. (A′′–E′′) Merged images. TUNEL-positive nuclei increased between 2 and 3 days after LIP and were still apparent at 5 or 7 days after LIP. In the last row (F, F′) a magnification of the damaged area 3 days after LIP shows DAPI counterstaining coincident with TUNEL signal. (A) The *small circle* (*white dotted line*) illustrates the small predetermined circular area →

←
(radius = 0.25 mm) centered in the lesion delimiting the TUNEL expression, that was analyzed in control (contralateral unexposed) and experimental retinas. (G) Percentage histogram of the positive TUNEL signal area within a small predetermined circular area at each timepoint studied (*statistical difference with the other groups; Tukey test $P < 0.001$). *Scale bar* (A′) = 100 μm. *Scale bar* (F) = 20 μm.

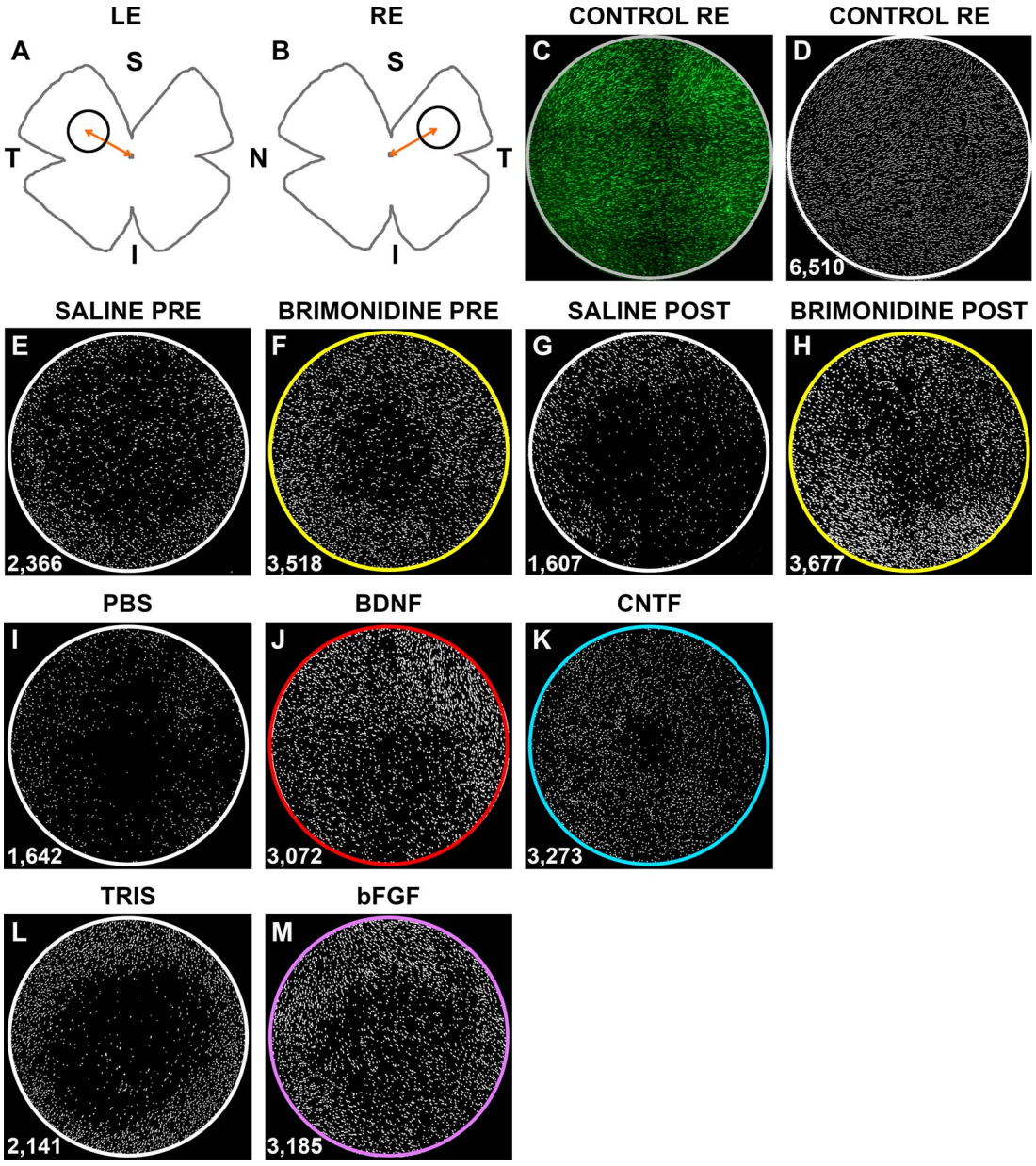

Figure 6. S-cone survival in the predetermined fixed-size circular areas after LIP and after different treatments. Representative examples of the predetermined fixed-size circular areas from control (A, B) and experimental (C, D) retinas after different treatments, including topical administration of Brimonidine before (F) and after (H) LIP and intravitreal administration of BDNF (J), CNTF (K), or bFGF (M) and its corresponding vehicles, saline (E, G), PBS (I), and TRIS (L), analyzed 7 days after LIP. For quantification, a predetermined fixed-size circular area (radius of 0.4 mm) was superimposed on the center of the lesion and S-opsin^{+}cones were quantified (A, B). The total number of S-cones counted in each predetermined fixed-size circular area is shown. Numbers of quantified S-cones are greater in the brimonidine, BDNF-, CNTF-, and bFGF-treated groups compared with their corresponding vehicle treated groups (E–M).

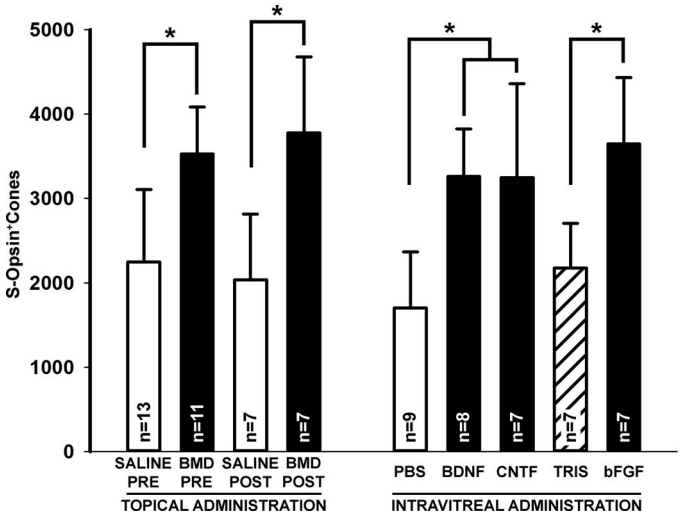

Figure 7. S-cone survival after different treatments. Bar graph showing S-cone survival 7 days after LIP and topical treatment with brimonidine pre- or post-LIP and intravitreal treatments with BDNF, CNTF, or bFGF and their corresponding vehicle solutions quantified within the predetermined fixed-size circular areas. Neuroprotection was afforded with all the used treatments. Kruskal–Wallis test $*P < 0.05$.

significantly with topical BMD or intravitreal administration of BDNF, bFGF, or CNTF.

LIP Results in a Consistent Focal Lesion Within the Superior-Temporal Retina

One goal of the study was to use an acute LED exposure to induce a reproducible and reliable focal lesion in the superior temporal region of the retina, where maximal visual sensitivity resides in the adult albino mice.[55] The in vivo (SD-OCT) analysis as well as the ex vivo retinal wholemount histologic analysis on the fluorescence and confocal microscope documented that LIP resulted in a focal lesion, with a radius of approximately 0.65 mm, consistently located in the superior-temporal quadrant with its center located at approximately 1.2 mm from the optic disc. This focal region exhibited a progressive thinning of the outer retina concomitant with the presence of apoptotic nuclei, infiltration of reactive microglia and a marked loss of S-opsin$^+$ cone outer segments.

Functional studies demonstrated transient alterations of the main a- and b-waves that recovered fully within 3 days and remain so by day 7. Thus, it is likely that the small focal LIP-induced lesion that affects cones and most likely also rods, does not result in significant permanent alterations of the main a- and b-waves of the ERG.

SD-OCT Analysis Indicated That LIP Induces Thinning of Outer Retinal Layers Within the Area of Lesion

It has been estimated that photoreceptors constitute 69.8%[79] to 82%[80] of the cells in pigmented mice retina, and that the total number of rods is approximately 6.4 million per retina whereas the total number of cones is of approximately 180,000 for pigmented[80] or 153,000 for albino[55] mice retina, and thus rods outnumber cones by approximately 34.7 times. In this study we have not directly examined rod photoreceptors, but the in vivo images of the SDOCT as well as the ex vivo images of the confocal microscopy suggest that within the area of lesion, a massive loss of cells occurs in the outer nuclear layer of the retina, which is predominantly occupied by rods. Indeed, the thinning of the retina, as measured with SD-OCT and observed with confocal microscopy, indicates that LIP affects mainly the outer nuclear and outer segment layers of the retina, and thus LIP affects not only the S-opsin$^+$ cones examined in our study but also rod-photoreceptors.

LIP Results in Focal Activation of Microglia Within the Area of Lesion

The retina presents a number of advantages for the study of central nervous system (CNS) functions,[73,74,81,82] including the role of microglia, a key component of the glial population in the CNS, during development, adulthood, and disease.[46,82,84,85] In healthy retinas microglial cells are mainly found in the inner retinal layers. During photoreceptors degeneration, microglia become activated and migrates to the outer retinal layer.[11,83] Confocal microscopic examination of the retinas at different time intervals after LIP allowed us to study in parallel the progressive loss of S-opsin$^+$ cone outer segments in the area of lesion as well as the increasing presence of Iba-1$^+$microglial cells and recruited macrophages. While on the naïve or control retinas, there were few to none Iba-1$^+$ cells within the outer nuclear and outer segment layer of the retina, in the experimental LIP treated retinas, a few Iba-1$^+$ cells were apparent in the outer retinal layers delimiting the area of the lesion by 1 day after LIP, and increased progressively thereafter until 7 days, reaching a peak at 3 days (Fig. 4). Microglial cells are known to play a crucial role in retinal degenerations,[85–88] specifically in photoreceptor degenerations,[83] where these immune cells became activated, change their morphology and migrate through the retina.[11,46,82–84] Indeed, microglial acti-

vation is an early event in photoreceptor degeneration and its inhibition increases photoreceptor survival,[46,83] thus it will be interesting to investigate whether inhibiting microglial activation results in larger survival of cones.[89]

LIP Results in Apoptotic Photoreceptor Cell Loss Within the Area of Lesion

This study uses S-opsin as a marker to identify the population of cones, and thus relies on the immune identification of S-opsin, but light-induced retinal damage may result in downregulation of proteins specific to retinal cell types (e.g., light-induced phototoxicity results in transient downregulation of the photopigment melanopsin).[23] Thus, it became important to determine if the disappearance of S-opsin$^+$ photoreceptors was the consequence of downregulation of the protein or cell death. TUNEL staining indicated that following LIP, the progressive loss of S-opsin$^+$ outer segments is probably not due to a downregulation of S-opsin but, at least in part, to apoptotic cell death within the outer layers of the retina. The presence of TUNEL$^+$ cells restricted to the small circular lesioned area of the retina confirmed that the injury induced in our setting was focal, and moreover constrained to the outer layers of the retina. Our results agree with previous studies indicating that following phototoxicity there is apoptotic cell death of photoreceptors.[90] Other studies that have investigated mechanisms involved in blue LED-induced photoreceptor cell death indicated that in addition to apoptosis there is necrotic death[90] accompanied by the presence of Iba-1$^+$ cells. Thus, it is possible that in our studies, necrotic photoreceptor death was present because we also observed Iba-1$^+$cells preferentially located within the circumscribed lesion. However, the present study was not designed to explore mechanisms involved in cone loss induced by LIP, but rather on the reliability and reproducibility of a mice model of focal phototoxicity in which to test neuroprotective strategies.

Topical BMD or Intravitreal Neurotrophic Factors Protect Against LIP-Induced Phototoxicity

The progressive TUNEL staining and parallel diminution in numbers of the S-opsin$^+$ outer segments, suggest that LIP induced S-cone photoreceptor loss is not only apoptotic but also a time-dependent progressive event. Thus, it was tempting to hypothesize that neuroprotective therapies at early time points after LIP could have an effective window for intervention. Indeed, neuroprotectants already known to have an effect in several types of retinal injury were tested, namely, alpha-2 selective agonists and the neurotrophic factors BDNF, CNTF, and bFGF.

The neuroprotective effects of alpha-2 selective agonists on the survival of retinal ganglion cells following transient ischemia or ocular hypertension of the retina have been widely studied.[42,43,91–94] Moreover, their effect on the survival of injured photoreceptors following phototoxicity is well established,[55,95] although their mechanism of action is still not fully understood.[68,96–98] Our results are consistent with our previous observations in an albino rat LIP model,[25] and document neuroprotection of S-opsin$^+$ cone photoreceptors afforded by topical BMD, when administered before or immediately after LIP exposure.

Trophic factors are endogenous substances with essential functions, such as promotion of proliferation, growth, regeneration, maturation, or neuronal survival.[99] Their neuroprotective role against photoreceptor degenerations are well known.[25,46,100–103] Moreover, a recent study documented the neuroprotective effects of CNTF or bFGF against photoreceptor degeneration in two inherited models of photoreceptor degeneration (P23H-1 rhodopsin mutation, and Royal College of Surgeons, pigment epithelium malfunction).[46] In accordance with these studies, our results show clear neuroprotective effects afforded by intravitreal administration of BDNF, CNTF, or bFGF against light-induced S-cone$^+$ photoreceptor cell loss. Thus, it is anticipated that this model could help to further understand photoreceptor survival and identify targets for effective neuroprotection in several retinal diseases coursing with photoreceptor cell loss.

Limitations of the Model

Our present studies have focused on the analysis of the S-opsin$^+$ cone photoreceptors. However, our OCT results also indicated that there is massive loss of rod photoreceptors. Thus although we have only analyzed S-cones, LIP clearly results in massive rod photoreceptor damage. Future studies using rod markers are required to characterize the effects of LIP on this photoreceptor population.

The morphologic results documented that LIP induces a small focal lesion of the retina, consistently located in the superior-temporal retina. The consistency of the location of the lesion in this model is an

advantage because it impinges upon the region of the retina that provides best visual acuity. However, the small size of the lesion requires a sophisticated quantitative analysis of a predetermined fixed-size circular area, centered in the lesion, to demonstrate the loss of S-opsin^{+} cone photoreceptors. Furthermore, the small size of the lesion is difficult to assess with functional or behavioral tests. Our attempt to characterize functional alterations with full-field ERG revealed no significant alterations, thus future studies using multifocal ERG are warranted to characterize this lesion. Moreover, it is likely that other visual behavioral test, such as optokinetic tracking or water maze will not detect abnormalities.

Overall, a detailed quantitative study of the population of S-cones following light-induced damage in adult albino mice had not been reported before. The present studies report that blue LED-induced phototoxicity is a reproducible, reliable, and quantifiable model of acute focal cone degeneration in which to study light-induced retinal degeneration longitudinally with noninvasive in vivo imaging techniques. Moreover, the model allows us to investigate quantitatively neuroprotection afforded by putative neuroprotectants on the population of S-cones. It is anticipated that this model may be used to design further strategies to protect photoreceptors against light-induced phototoxicity.

Acknowledgments

We thank W. M. Bloss, S.A. Barcelona, Spain for providing the SD-OCT.

Supported by grants from Fundación Séneca, Agencia de Ciencia y Tecnología Región de Murcia (19881/GERM/15), and the Spanish Ministry of Economy and Competitiveness, Instituto de Salud Carlos III, Fondo Europeo de Desarrollo Regional "Una Manera de Hacer Europa" (SAF2015-67643-P, PI16/00380, RD16/0008/0026), and Allergan Inc., unrestricted grant to MV-S.

Presented at the annual meeting of the Association for Research in Vision and Ophthalmology (Orlando, Florida, May 2015) Vidal-Sanz M, et al., *IOVS* 2015;55:ARVO E-Abstract 5667.

Disclosure: **F.J. Valiente-Soriano**, None; **A. Ortín-Martínez**, None; **J. Di Pierdomenico**, None; **D. García-Ayuso**, None; **A. Gallego-Ortega**, None; **J.A. Miralles de Imperial-Ollero**; None; **M. Jiménez-López**, None; **M.P. Villegas-Pérez**, None; **L.A. Wheeler**, None; **M. Vidal-Sanz**, None

*Francisco J. Valiente-Soriano and Arturo Ortín-Martínez are joint first authors.

References

1. Klein R, Cruickshanks KJ, Nash SD, et al. The prevalence of age-related macular degeneration and associated risk factors. *Arch Ophthalmol*. 2010;128:750–758.
2. Sui GY, Liu GC, Liu GY, et al. Is sunlight exposure a risk factor for age-related macular degeneration? A systematic review and meta-analysis. *Br J Ophthalmol*. 2013;97:389–394.
3. Srivastava P, Sinha-Mahapatra SK, Ghosh A, Srivastava I, Dhingra NK. Differential alterations in the expression of neurotransmitter receptors in inner retina following loss of photoreceptors in rd1 mouse. *PLoS One*. 2015; 10:e0123896.
4. Gargini C, Terzibasi E, Mazzoni F, Strettoi E. Retinal organization in the retinal degeneration 10 (rd10) mutant mouse: a morphological and ERG study. *J Comp Neurol*. 2007;500:222–238.
5. Rösch S, Aretzweiler C, Müller F, Walter P. Evaluation of retinal function and morphology of the pink-eyed Royal College of Surgeons (RCS) rat: a comparative study of in vivo and in vitro methods. *Curr Eye Res*. 2017;42:273–281.
6. Ryals RC, Andrews MD, Datta S, et al. Long-term characterization of retinal degeneration in Royal College of Surgeons rats using spectral-domain optical coherence tomography. *Invest Ophthalmol Vis Sci*. 2017;58:1378–1386.
7. García-Ayuso D, Salinas-Navarro M, Agudo M, et al. Retinal ganglion cell numbers and delayed retinal ganglion cell death in the P23H rat retina. *Exp Eye Res*. 2010;91:800–810.
8. García-Ayuso D, Salinas-Navarro M, Nadal-Nicolás FM, et al. Sectorial loss of retinal ganglion cells in inherited photoreceptor degeneration is due to RGC death. *Br J Ophthalmol*. 2014;98:396–401.
9. Wang S, Villegas-Pérez MP, Vidal-Sanz M, Lund RD. Progressive optic axon dystrophy and vascular changes in rd mice. *Invest Ophthalmol Vis Sci*. 2000;41:537–545.
10. Wang S, Villegas-Pérez MP, Holmes T, et al. Evolving neurovascular relationships in the RCS rat with age. *Curr Eye Res*. 2003;27:183–196.

11. Di Pierdomenico J, García-Ayuso D, Pinilla I, et al. Early events in retinal degeneration caused by rhodopsin mutation or pigment epithelium malfunction: differences and similarities. *Front Neuroanat*. 2017;11:14.
12. Villegas-Pérez MP, Vidal-Sanz M, Lund RD. Mechanism of retinal ganglion cell loss in inherited retinal dystrophy. *Neuroreport*. 1996; 7:1995–1999.
13. Villegas-Pérez MP, Lawrence JM, Vidal-Sanz M, Lavail MM, Lund RD. Ganglion cell loss in RCS rat retina: a result of compression of axons by contracting intraretinal vessels linked to the pigment epithelium. *J Comp Neurol*. 1998;392: 58–77.
14. Sorsby A. Experimental pigmentary degeneration of the retina by sodium iodate. *Br J Ophthalmol*. 1941;25:58–62.
15. Kannan R, Hinton DR. Sodium iodate induced retinal degeneration: new insights from an old model. *Neural Regen Res*. 2014;9:2044–2045.
16. Chowers G, Cohen M, Marks-Ohana D, et al. Course of sodium iodate-induced retinal degeneration in albino and pigmented mice. *Invest Ophthalmol Vis Sci*. 2017;58:2239–2249.
17. Wang J, Iacovelli J, Spencer C, Saint-Geniez M. Direct effect of sodium iodate on neurosensory retina. *Invest Ophthalmol Vis Sci*. 2014;55:1941–1953.
18. Herrold KM. Pigmentary degeneration of the retina induced by N-methyl-N-nitrosourea. An experimental study in Syrian hamsters. *Arch Ophthalmol*. 1967;78:650–653.
19. Emoto Y, Yoshizawa K, Kinoshita Y, Yuki M, Yuri T, Tsubura A. Susceptibility to N-methyl-N-nitrosourea-induced retinal degeneration in different rat strains. *J Toxicol Pathol*. 2015;29: 67–71.
20. Noell WK, Walker VS, Kang BS, Berman S. Retinal damage by light in rats. *Invest Ophthalmol*. 1966;5:450–473.
21. Marco-Gomariz MA, Hurtado-Montalbán N, Vidal-Sanz M, Lund RD, Villegas-Pérez MP. Phototoxic-induced photoreceptor degeneration causes retinal ganglion cell degeneration in pigmented rats. *J Comp Neurol*. 2006;498:163–179.
22. García-Ayuso D, Salinas-Navarro M, Agudo-Barriuso M, Alarcón-Martínez L, Vidal-Sanz M, Villegas-Pérez MP. Retinal ganglion cell axonal compression by retinal vessels in light-induced retinal degeneration. *Mol Vis*. 2011;17: 1716–1733.
23. García-Ayuso D, Galindo-Romero C, Di Pierdomenico J, Vidal-Sanz M, Agudo-Barriuso M, Villegas Pérez MP. Light-induced retinal degeneration causes a transient downregulation of melanopsin in the rat retina. *Exp Eye Res*. 2017; 161:10–16.
24. Montalbán-Soler L, Alarcón-Martínez L, Jiménez-López M, et al. Retinal compensatory changes after light damage in albino mice. *Mol Vis*. 2012;18:675–693.
25. Ortín-Martínez A, Valiente-Soriano FJ, García-Ayuso D, et al. A novel in vivo model of focal light emitting diode-induced cone-photoreceptor phototoxicity: neuroprotection afforded by brimonidine, BDNF, PEDF or bFGF. *PLoS One*. 2014;9:e113798.
26. Kim GH, Kim HI, Paik SS, Jung SW, Kang S, Kim IB. Functional and morphological evaluation of blue light-emitting diode-induced retinal degeneration in mice. *Graefes Arch Clin Exp Ophthalmol*. 2016;254:705–716.
27. Nakamura M, Yako T, Kuse Y, et al. Exposure to excessive blue LED light damages retinal pigment epithelium and photoreceptors of pigmented mice. *Exp Eye Res*. 2018;177:1–11.
28. Krigel A, Berdugo M, Picard E, et al. Light-induced retinal damage using different light sources, protocols and rat strains reveals LED phototoxicity. *Neuroscience*. 2016;339:296–307.
29. Chen E. Inhibition of cytochrome oxidase and blue-light damage in rat retina. *Graefes Arch Clin Exp Ophthalmol*. 1993;231:416–423.
30. Cai J, Nelson KC, Wu M, Sternberg P Jr, Jones DP. Oxidative damage and protection of the RPE. *Prog Retin Eye Res*. 2000;19:205–221.
31. Kuse Y, Ogawa K, Tsuruma K, Shimazawa M, Hara H. Damage of photoreceptor-derived cells in culture induced by light emitting diode-derived blue light. *Sci Rep*. 2014;4:5223.
32. Jarrett SG, Boulton ME. Consequences of oxidative stress in age-related macular degeneration. *Mol Aspects Med*. 2012;33:399–417.
33. Liang FQ, Godley BF. Oxidative stress-induced mitochondrial DNA damage in human retinal pigment epithelial cells: a possible mechanism for RPE aging and age-related macular degeneration. *Exp Eye Res*. 2003;76:397–403.
34. Sparrow JR, Nakanishi K, Parish CA. The lipofuscin fluorophore A2E mediates blue light-induced damage to retinal pigmented epithelial cells. *Invest Ophthalmol Vis Sci*.41:1981–1989.
35. Nakamura M, Kuse Y, Tsuruma K, Shimazawa M, Hara H. The involvement of the oxidative

stress in murine blue LED light-induced retinal damage model. *Biol Pharm Bull*. 2017;40:1219–1225.
36. Vidal-Sanz M, Galindo-Romero C, Valiente-Soriano FJ, et al. Shared and differential retinal responses against optic nerve injury and ocular hypertension. *Front Neurosci*. 2017;11:235.
37. Jehle T, Dimitriu C, Auer S, et al. The neuropeptide NAP provides neuroprotection against retinal ganglion cell damage after retinal ischemia and optic nerve crush. *Graefes Arch Clin Exp Ophthalmol*. 2008;246:1255–1263.
38. Lindqvist N, Peinado-Ramón P, Vidal-Sanz M, Hallböök F. GDNF, Ret, GFRalpha1 and 2 in the adult rat retino-tectal system after optic nerve transection. *Exp Neurol*. 2004;187:487–499.
39. Sánchez-Migallón MC, Valiente-Soriano FJ, Salinas-Navarro M, et al. Nerve fibre layer degeneration and retinal ganglion cell loss long term after optic nerve crush or transection in adult mice. *Exp Eye Res*. 2018;170:40–50.
40. Vidal-Sanz M, Lafuente M, Sobrado-Calvo P, et al. Death and neuroprotection of retinal ganglion cells after different types of injury. *Neurotox Res*. 2000;2:215–227.
41. Vidal-Sanz M, de la Villa P, Avilés-Trigueros M, et al. Neuroprotection of retinal ganglion cell function and their central nervous system targets. *Eye*. 2007;21:42–45.
42. Avilés-Trigueros M, Mayor-Torroglosa S, García-Avilés A, et al. Transient ischemia of the retina results in massive degeneration of the retinotectal projection: long-term neuroprotection with brimonidine. *Exp Neurol*. 2003;184:767–777.
43. Mayor-Torroglosa S, De la Villa P, Rodríguez ME, et al. Ischemia results 3 months later in altered ERG, degeneration of inner layers, and deafferented tectum: neuroprotection with brimonidine. *Invest Ophthalmol Vis Sci*. 2005;46:3825–3835.
44. Valiente-Soriano FJ, Nadal-Nicolás FM, Salinas-Navarro M, et al. BDNF rescues RGCs but not intrinsically photosensitive RGCs in ocular hypertensive albino rat retinas. *Invest Ophthalmol Vis Sci*. 2015;56:1924–1936.
45. Rovere G, Nadal-Nicolás FM, Wang J, et al. Melanopsin-containing or non-melanopsin-containing retinal ganglion cells response to acute ocular hypertension with or without brain-derived neurotrophic factor neuroprotection. *Invest Ophthalmol Vis Sci*. 2016;57:6652–6661.
46. Di Pierdomenico J, Scholz R, Valiente-Soriano FJ, et al. Neuroprotective effects of FGF2 and minocycline in two animal models of inherited retinal degeneration. *Invest Ophthalmol Vis Sci*. 2018;59:4392–4403.
47. García-Ayuso D, Di Pierdomenico J, Agudo-Barriuso M, Vidal-Sanz M, Villegas-Pérez MP. Retinal remodeling following photoreceptor degeneration causes retinal ganglion cell death. *Neural Regen Res*. 2018;13:1885–1886.
48. Wen R, Tao W, Li Y, Sieving PA. CNTF and retina. *Prog Retin Eye Res*. 2012;31:136–151.
49. Lafuente MP, Villegas-Pérez MP, Mayor S, Aguilera ME, Miralles de Imperial J, Vidal-Sanz M. Neuroprotective effects of brimonidine against transient ischemia-induced retinal ganglion cell death: a dose response in vivo study. *Exp Eye Res*. 2002;74:181–189.
50. Lafuente López-Herrera MP, Mayor-Torroglosa S, Miralles de Imperial J, Villegas-Pérez MP, Vidal-Sanz M. Transient ischemia of the retina results in altered retrograde axoplasmic transport: neuroprotection with brimonidine. *Exp Neurol*. 2002;178:243–258.
51. Salinas-Navarro M, Mayor-Torroglosa S, Jiménez-López M, et al. A computerized analysis of the entire retinal ganglion cell population and its spatial distribution in adult rats. *Vision Res*. 2009;49:115–126.
52. Salinas-Navarro M, Jiménez-López M, Valiente-Soriano FJ, et al. Retinal ganglion cell population in adult albino and pigmented mice: a computerized analysis of the entire population and its spatial distribution. *Vision Res*. 2009;49:637–647.
53. Nadal-Nicolás FM, Jiménez-López M, Sobrado-Calvo P, et al. Brn3a as a marker of retinal ganglion cells: qualitative and quantitative time course studies in naive and optic nerve-injured retinas. *Invest Ophthalmol Vis Sci*. 2009;50:3860–3868.
54. Ortín-Martínez A, Jiménez-López M, Nadal-Nicolás FM, et al. Automated quantification and topographical distribution of the whole population of S- and L-cones in adult albino and pigmented rats. *Invest Ophthalmol Vis Sci*. 2010;51:3171–3183.
55. Ortín-Martínez A, Nadal-Nicolás FM, Jiménez-López M, et al. Number and distribution of mouse retinal cone photoreceptors: differences between an albino (Swiss) and a pigmented (C57/BL6) strain. *PLoS One*. 2014;9:e102392.

56. Ortín-Martínez A, Salinas-Navarro M, Nadal-Nicolás FM, et al. Laser-induced ocular hypertension in adult rats does not affect non-RGC neurons in the ganglion cell layer but results in protracted severe loss of cone-photoreceptors. *Exp Eye Res*. 2015;132:17–33.
57. Organisciak DT, Darrow RA, Barsalou L, Darrow RM, Lininger LA. Light-induced damage in the retina: differential effects of dimethylthiourea on photoreceptor survival, apoptosis and DNA oxidation. *Photochem Photobiol*. 1999;70:261–268.
58. Remé CE, Hafezi F, Munz K, Reinboth J. Light damage to retina and pigment epithelium. In: Marmor MF, Wolfensberger TJ, eds. *The Retinal Pigment Epithelium: Current Aspects of Function and Disease*: Oxford University Press; Oxford UK; 1998:563–586.
59. Williams TP, Howell WL. Action spectrum of retinal light-damage in albino rats. *Invest Ophthalmol Vis Sci*. 1983;24:285–287.
60. Glickman RD. Phototoxicity to the retina: mechanisms of damage. *Int J Toxicol*. 2002;21:473–490.
61. Vaughan DK, Nemke JL, Fliesler SJ, Darrow RM, Organisciak DT. Evidence for a circadian rhythm of susceptibility to retinal light damage. *Photochem Photobiol*. 2002;75:547–553.
62. Algvere PV, Marshall J, Seregard S. Age-related maculopathy and the impact of blue light hazard. *Acta Ophthalmol Scand*. 2006;84:4–15.
63. Organisciak DT, Vaughan DK. Retinal light damage: mechanisms and protection. *Prog Retin Eye Res*. 2010;29:113–134.
64. Alarcón-Martínez L, de la Villa P, Avilés-Trigueros M, Blanco R, Villegas-Pérez MP, Vidal-Sanz M. Short and long term axotomy-induced ERG changes in albino and pigmented rats. *Mol Vis*. 2009;15:2373–2383.
65. Alarcón-Martínez L, Avilés-Trigueros M, Galindo-Romero C, et al. ERG changes in albino and pigmented mice after optic nerve transection. *Vision Res*. 2010;50:2176–2187.
66. Sánchez-Migallón MC, Valiente-Soriano FJ, Nadal-Nicolás FM, Vidal-Sanz M, Agudo-Barriuso M. Apoptotic retinal ganglion cell death after optic nerve transection or crush in mice: delayed RGC loss with BDNF or a caspase 3 inhibitor. *Invest Ophthalmol Vis Sci*. 2016;57:81–93.
67. Parrilla-Reverter G, Agudo M, Nadal-Nicolás F, et al. Time-course of the retinal nerve fibre layer degeneration after complete intra-orbital optic nerve transection or crush: a comparative study. *Vision Res*. 2009;49:2808–2825.
68. Lönngren U, Näpänkangas U, Lafuente M, et al. The growth factor response in ischemic rat retina and superior colliculus after brimonidine pre-treatment. *Brain Res Bull*. 2006;71:208–218.
69. Nadal-Nicolás FM, Jiménez-López M, Salinas-Navarro M, et al. Whole number, distribution and co-expression of brn3 transcription factors in retinal ganglion cells of adult albino and pigmented rats. *PLoS One*. 2012;7:e49830.
70. Nadal-Nicolás FM, Salinas-Navarro M, Vidal-Sanz M, Agudo-Barriuso M. Two methods to trace retinal ganglion cells with fluorogold: from the intact optic nerve or by stereotactic injection into the optic tract. *Exp Eye Res*. 2015;131:12–19.
71. Valiente-Soriano FJ, García-Ayuso D, Ortín-Martínez A, et al. Distribution of melanopsin positive neurons in pigmented and albino mice: evidence for melanopsin interneurons in the mouse retina. *Front Neuroanat*. 2014;8:131.
72. Valiente-Soriano FJ, Salinas-Navarro M, Jiménez-López M, et al. Effects of ocular hypertension in the visual system of pigmented mice. *PLoS One*. 2015;10:e0121134.
73. Vidal-Sanz M, Nadal-Nicolás FM, Valiente-Soriano FJ, Agudo-Barriuso M, Villegas-Pérez MP. Identifying specific RGC types may shed light on their idiosyncratic responses to neuroprotection. *Neural Regen Res*. 2015;10:1228–1230.
74. Vidal-Sanz M, Valiente-Soriano FJ, Ortín-Martínez A, et al. Retinal neurodegeneration in experimental glaucoma. *Prog Brain Res*. 2015;220:1–35.
75. García-Ayuso D, Ortín-Martínez A, Jiménez-López M, et al. Changes in the photoreceptor mosaic of P23H-1 rats during retinal degeneration: implications for rod-cone dependent survival. *Invest Ophthalmol Vis Sci*. 2013;54:5888–5900.
76. Pennesi ME, Michaels KV, Magee SS, et al. Long-term characterization of retinal degeneration in rd1 and rd10 mice using spectral domain optical coherence tomography. *Invest Ophthalmol Vis Sci*. 2012;53:4644–4656.
77. DiCicco RM, Bell BA, Kaul C, et al. Retinal regeneration following OCT-guided laser injury in zebrafish. *Invest Ophthalmol Vis Sci*. 2014;55:6281–6288.
78. Massengill MT, Young B, Patel D, et al. Clinically relevant outcome measures for the

I307N rhodopsin mouse: a model of inducible autosomal dominant retinitis pigmentosa. *Invest Ophthalmol Vis Sci*. 2018;59:5417–5430.
79. Macosko EZ, Basu A, Satija R, et al. Highly parallel genome-wide expression profiling of individual cells using nanoliter droplets. *Cell*. 2015;161:1202–1214.
80. Jeon CJ, Strettoi E, Masland RH. The major cell populations of the mouse retina. *J Neurosci*. 1998;18:8936–8946.
81. Vidal-Sanz M, Salinas-Navarro M, Nadal-Nicolás FM, et al. Understanding glaucomatous damage: anatomical and functional data from ocular hypertensive rodent retinas. *Prog Retin Eye Res*. 2012;31:1–27.
82. Silverman SM, Wong WT. Microglia in the retina: roles in development, maturity, and disease. *Annu Rev Vis Sci*. 2018;4:45–77.
83. Di Pierdomenico J, García-Ayuso D, Agudo-Barriuso M, Vidal-Sanz M, Villegas-Pérez MP. Role of microglial cells in photoreceptor degeneration. *Neural Regen Res*. 2019;14:1186–1190.
84. Langmann T. Microglia activation in retinal degeneration. *J Leukoc Biol*. 2007;81:1345–1351.
85. Sobrado-Calvo P, Vidal-Sanz M, Villegas-Pérez MP. Rat retinal microglial cells under normal conditions, after optic nerve section, and after optic nerve section and intravitreal injection of trophic factors or macrophage inhibitory factor. *J Comp Neurol*. 2007;501:866–878.
86. de Hoz R, Gallego BI, Ramírez AI, et al. Rod-like microglia are restricted to eyes with laser-induced ocular hypertension but absent from the microglial changes in the contralateral untreated eye. *PLoS One*. 2013;8:e83733.
87. de Hoz R, Ramírez AI, González-Martín R, et al. Bilateral early activation of retinal microglial cells in a mouse model of unilateral laser-induced experimental ocular hypertension. *Exp Eye Res*. 2018;171:12–29.
88. Salvador-Silva M, Vidal-Sanz M, Villegas-Pérez MP. Microglial cells in the retina of Carassius auratus: effects of optic nerve crush. *J Comp Neurol*. 2000;417:431–447.
89. Mages K, Grassmann F, Jägle H, et al. The agonistic TSPO ligand XBD173 attenuates the glial response thereby protecting inner retinal neurons in a murine model of retinal ischemia. *J Neuroinflammation*. 2019;16:43.
90. Jaadane I, Boulenguez P, Chahory S, et al. Retinal damage induced by commercial light emitting diodes (LEDs). *Free Radic Biol Med*. 2015;84:373–384.
91. Wheeler L, WoldeMussie E, Lai R. Role of alpha-2 agonists in neuroprotection. *Surv Ophthalmol*. 2003;48:47–51.
92. Saylor M, McLoon LK, Harrison AR, Lee MS. Experimental and clinical evidence for brimonidine as an optic nerve and retinal neuroprotective agent: an evidence-based review. *Arch Ophthalmol*. 2009;127:402–406.
93. Kusari J, Zhou SX, Padillo E, Clarke KG, Gil DW. Inhibition of vitreoretinal VEGF elevation and blood-retinal barrier breakdown in streptozotocin-induced diabetic rats by brimonidine. *Invest Ophthalmol Vis Sci*. 2010;51:1044–1051.
94. Kusari J, Padillo E, Zhou SX, et al. Effect of brimonidine on retinal and choroidal neovascularization in a mouse model of retinopathy of prematurity and laser-treated rats. *Invest Ophthalmol Vis Sci*. 2011;52:5424–5431.
95. Wen R, Cheng T, Li Y, Cao W, Steinberg RH. Alpha 2-adrenergic agonists induce basic fibroblast growth factor expression in photoreceptors in vivo and ameliorate light damage. *J Neurosci*. 1996;16:5986–5992.
96. Gao H, Qiao X, Cantor LB, WuDunn D. Up-regulation of brain-derived neurotrophic factor expression by brimonidine in rat retinal ganglion cells. *Arch Ophthalmol*. 2002;120:797–803.
97. Peng M, Li Y, Luo Z, et al. Alpha2-adrenergic agonists selectively activate extracellular signal-regulated kinases in Müller cells in vivo. *Invest Ophthalmol Vis Sci*. 1998;39:1721–1726.
98. Harun-Or-Rashid M, Lindqvist N, Hallböök F. Transactivation of EGF receptors in chicken Müller cells by α2A-adrenergic receptors stimulated by brimonidine. *Invest Ophthalmol Vis Sci*. 2014;55:3385–3394.
99. Kolomeyer AM, Zarbin MA. Trophic factors in the pathogenesis and therapy for retinal degenerative diseases. *Surv Ophthalmol*. 2014;59:134–165.
100. Faktorovich EG, Steinberg RH, Yasumura D, Matthes MT, LaVail MM. Photoreceptor degeneration in inherited retinal dystrophy delayed by basic fibroblast growth factor. *Nature*. 1990;347:83–86.
101. Green ES, Rendahl KG, Zhou S, et al. Two animal models of retinal degeneration are rescued by recombinant adeno-associated virus-mediated production of FGF-5 and FGF-18. *Mol Ther*. 2001;3:507–515.

102. Miyazaki M, Ikeda Y, Yonemitsu Y, et al. Simian lentiviral vector-mediated retinal gene transfer of pigment epithelium-derived factor protects retinal degeneration and electrical defect in Royal College of Surgeons rats. *Gene Ther*. 2003;10:1503–1511.

103. Buch PK, MacLaren RE, Duran Y, et al. In contrast to AAV-mediated Cntf expression, AAV-mediated Gdnf expression enhances gene replacement therapy in rodent models of retinal degeneration. *Mol Ther*. 2006;14:700–709.